Proceedings of the International Workshop on Quasiconformal
Mappings and their Applications (IWQCMA05)

History and Recent Developments in Techniques for Numerical Conformal Mapping

R. Michael Porter

Abstract. A brief outline is given of some of the main historical developments in the theory and practice of conformal mappings. Originating with the science of cartography, conformal mappings has given rise to many highly sophisticated methods. We emphasize the principles of mathematical discovery involved in the development of numerical methods, through several examples.

Keywords. numerical conformal mapping, cartography, osculation, interpolating polynomial method, mathematical discovery.

2000 MSC. 65-03 30C30 65-02 65S05.

Contents

Research supported by CONACyt grant 46936.

1. Introduction

Although the present meeting is mainly concerned with the study of the theory of quasiconformal mapping, our topic here is to understand some of the basic principles of the theory of *conformal* mapping, with emphasis on the computational perspective.

The history of quasiconformal mappings is usually traced back to the early 1800's with a solution by C. F. Gauss to a problem which will be briefly mentioned at the end of Section 2, while conformal mapping goes back to the ideas of G. Mercator in the 16th century. Since the early work had much to do with the production of maps of the physical world, we will begin with a brief survey of how this came about.

2. A Brief History of Mapmaking

From antiquity mankind has needed to map out his world: whether for controlling dominated territories or to travel great distances. For the moment, by *map* we will mean a representation of part of the earth's surface on a flat paper. Indeed, as one historian writes, mapmaking is older than the written word:

> "The human activity of graphically translating one's perception of his world is now generally recognized as a universally acquired skill and one that pre-dates virtually all other forms of written communication."[1]

A map obviously must contain "known reference points" and somehow show their relative distances and directions. This is the basis of the humor in the following lines from "The Hunting of the Snark" by Lewis Carroll,

[1] `www.henry-davis.com/MAPS/AncientWebPages/100mono.html`. As with many of the web references cited here, the same information may be found on many sites and it is difficult to pinpoint an original source.

FIGURE 1. "Map" lacking reference points

He had bought a large map[2] representing the sea,
Without the least vestige of land:
And the crew were much pleased when they found it to be
A map they could all understand.

"What's the good of Mercator's North Poles and Equators,
Tropics, Zones, and Meridian Lines?"
So the Bellman would cry: and the crew would reply
"They are merely conventional signs!"

"Other maps are such shapes, with their islands and capes!
But we've got our brave Captain to thank"
(So the crew would protest) "that he's bought us the best
A perfect and absolute blank!"

[2]http://www.eq5.net/carrol/fit2.html

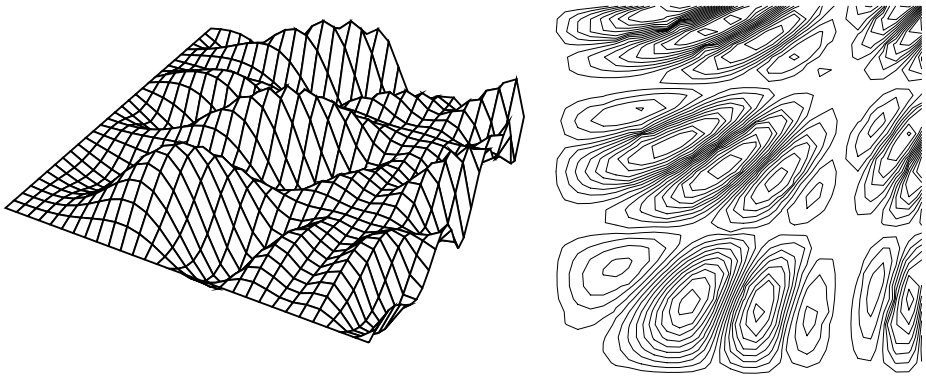

FIGURE 2. Left: Perspective view of terrain. Right: Topographical map of same terrain.

FIGURE 3. Right: Reconstruction of Catalhoyuk map, which is said to have had the function of registering property ownership.

The picture of a terrain in Figure 2 (left) is likewise not a map. In the map of Figure 2 (right), the reference points are "subjective," involving loci of constant height which need not correspond to any physically noticeable characteristics of the terrain. Maps may incorporate our preconceptions or prejudices of what the world looks like.

Of course, in modern mathematics the matter of reference points is resolved by the precise notion "function," for which it is postulated that *every* point of the surface is made to correspond, albeit theoretically, to a unique point of the map.

Let us take a quick trip though the history of maps. A nine-foot-long stone map dating from 6200 B.C., which appears to be a plan of a town predating Ankara, Turkey[3], is shown in Figure 3. It is said to have served to register property rights, perhaps for tax purposes.

Moving now to larger-scale maps, we have a map of Africa produced in silk, in 1389 by the Chinese map Great Ming Empire), measuring 17 square meters (Figure 4). It is on display in South Africa and is said to be a copy of an earlier stone one[4]. However, it would be a mistake to say that the larger the scale, the more recent the map. In 1999 there was discovered in Ireland a map dating from

[3]John F. Brock, "The Oldest Cadastral Plan Ever Found: the Catalhoyuk town plan of 6200 B.C.," `http://www.mash.org.au/articles/articles2.htm`

[4]BBC News, `http://news.bbc.co.uk/2/hi/africa/2446907.stm`

FIGURE 4. Chinese map of Africa

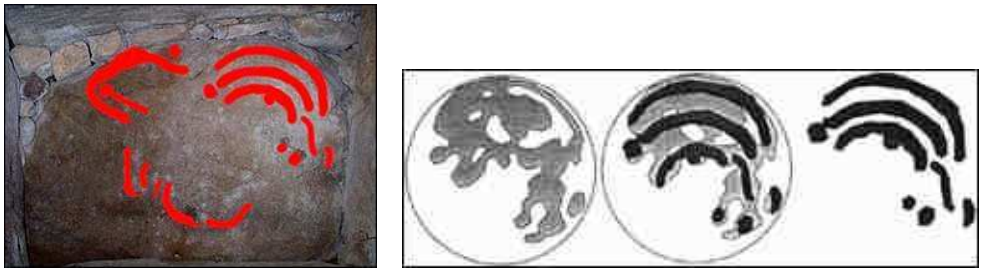

FIGURE 5. Alleged ancient moon map

about 3000 B.C. which is claimed to be the oldest known map of the moon.[5] Even older are the well-known drawings in from 14,000 B.C the Lascaux Caves, France, discovered in 1940, with a drawing of the constellation Pleiades and of the "Summer Triangle," and a map of the constellation Orion from 30,000 B.C. found engraved on a 4 cm. ivory tablet in Germany in 1979.[6]

At the time of this writing, it is being investigated whether or not the Chinese admiral Zheng He discovered America and circled the globe 80 years before the voyages of Christopher Columbus; part of the argument is based on a map from the year 1418.[7] At any rate, it is often stated incorrectly that in the epoch of Columbus, people generally thought that the earth was flat. While the spherical nature of the earth's surface was known to the ancient Greeks, and its diameter was measured by Hipparcus (190–120 A.C.), it is significant that no early map was produced similar to that of Figure 6.

The principle here is that consciously or not, one tends to look for the simplest possible answers to mathematical questions. Here it would be the *topology* which is unnecessarily complicated. The possibility of closed curves on the earth's

[5] `http://news.bbc.co.uk/1/hi/sci/tech/1205638.stm`

[6] `http://news.bbc.co.uk/1/hi/sci/tech/871930.stm` and `http://news.bbc.co.uk/1/hi/sci/tech/2679675.stm`

[7] *The Sunday Statesman*, New Delhi, 15 January, 2006; `http://edition.cnn.com/2003/SHOWBIZ/books/01/13/1421/index.html`

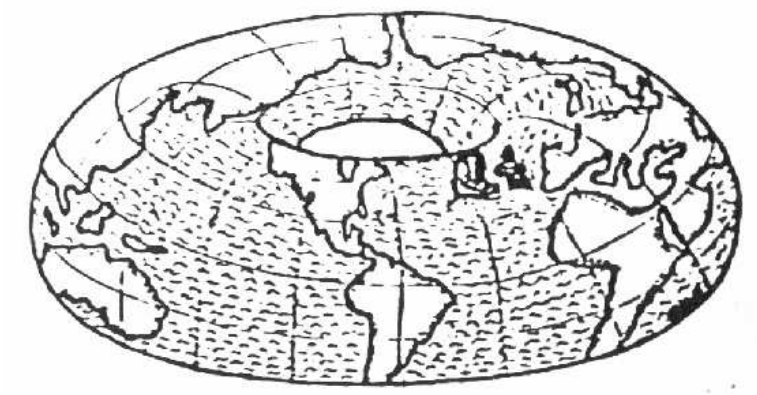

FIGURE 6.

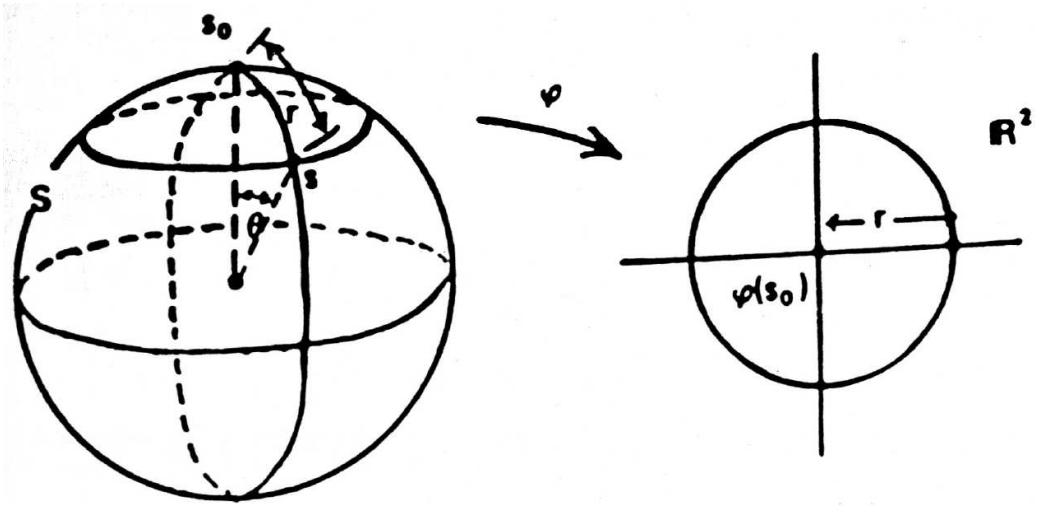

FIGURE 7. If there were an isometry ϕ from a neighborhood of the North Pole to a planar region, then circles of radius r in the two spaces would have different circumferences.

surface which are not contractible to a point would have many consequences, among them a nonconstant curvature of the surface (at least according to our intuitive notions of Euclidean space).

So let us return to the idea of a spherical earth. The oldest known maps of the celestial sphere were not on flat surfaces such as paper, but rather on tortoise shells. One reason for this may have been that, as Figure 7 shows, *there can be no isometry (that is, a distance-preserving map) from a spherical region to a planar one.*

This statement may sound disappointing, because it would be extremely useful to be able to determine one's position on a map using the distance one has traveled from a previously determined point. However, navigators of the Middle Ages realized that if *distances* cannot be preserved on planar maps of spherical surfaces, then at least it would be useful to conserve *angles.* When the angles between curves on the earth are equal to the corresponding angles on the map, the map is said to be *conformal* (Figure 8). A navigator on the high seas, orienting

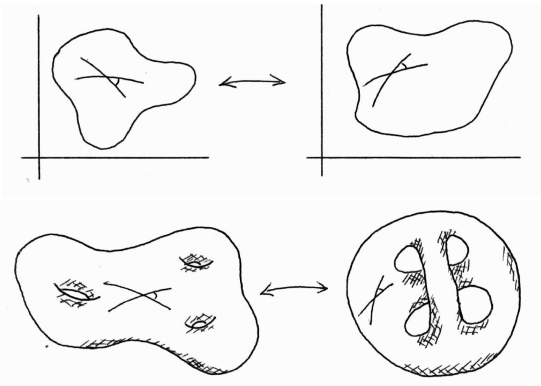

FIGURE 8. Conformal mapping of plane domains and of surfaces.

himself by the stars, has to go through some rather involved calculations to determine the distance he has just traveled. However, the stars tell him quickly the *direction* in which he is traveling, and hence the angle which his course is making with lines of latitude and longitude. Thus a conformal (nonisometric) map is not necessarily as impractical as it may first seem.

As is mentioned also in A. Rasila's article, the idea of a conformal earth map was developed by G. Mercator. The map is designed in two steps. The first step is to project all points of the sphere except the poles to a cylinder in which the sphere is inscribed (Figure 9). Then the horizontal lines in the image are to be adjusted, placing the line corresponding to latitude θ at the height $\varphi(\theta)$. Mercator did not know how to do this second step precisely; it was E. Wright in 1599 who found the theoretical solution,

$$\varphi(\theta) = \int_0^\theta \frac{d\theta}{\cos\theta}.$$

At that time no one knew how to evaluate this integral in elementary terms. This led to the compilation of numerical tables for navigators, which was carried out by successively summing small increments of the integrand. After some time, people compared different tables and observed a curious coincidence: the integral

$$\int_0^\theta \frac{d\theta}{\cos\theta}$$

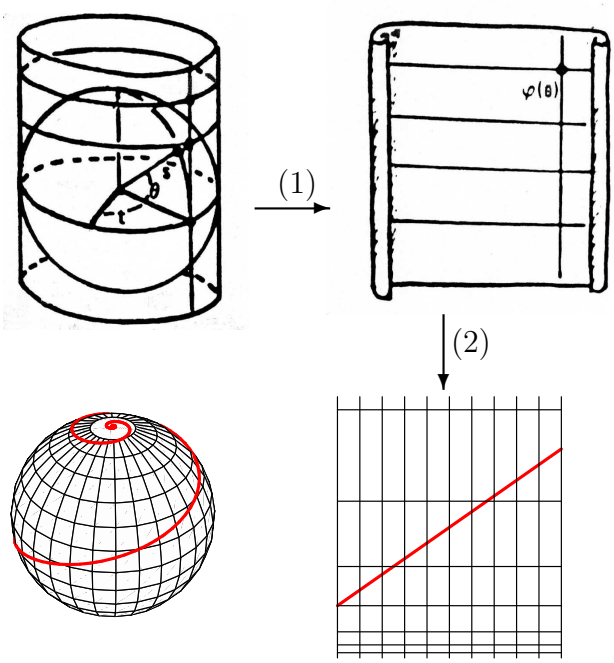

FIGURE 9. Steps in Mercator projection

was apparently approximately equal to

$$\log\ \tan\Big(\frac{\theta}{2}+\frac{\pi}{4}\Big),$$

a statement which became a conjecture and was finally proved in 1668 by J. Gregory.

The point of this rather long digression is to illustrate that the interplay between "pure" and "applied" mathematics has been with us for a long time. Numerical evidence has long played an important role in the generation of conjectures and theorems; leaving aside questions arising from ancient geodesy, we mention only the Prime Number Theorem conjectured by Gauss, and the location of zeroes of the zeta function known as the Riemann Hypothesis.

Let us look again at Figure 8. The problem of finding a conformal correspondence between an arbitrary region and a plane region is rather complicated, and classically is called the problem of finding isothermic coordinates for a surface. For real-analytic surfaces, this was solved by Gauss. The solution requires quasiconformal mappings as an intermediate step, and will not be explained in detail here.

3. The General Problem of Conformal Mappings

Here we limit the discussion to plane domains. From the theory of functions of a Complex Variable we have the following basic fact.

> *A correspondence f between plane domains is* conformal *if and only if it can be represented locally as an* analytic *function of a complex variable $z = x + iy$,*
>
> $$f(z) = \sum_0^\infty a_k (z - z_0)^k.$$

Thus, once a conformal mapping is found from a given surface to a plane region, all other conformal mappings are obtained from this one by composing with an analytic function.

Applications of conformal mapping to physics, too numerous to mention here, require finding conformal mappings between two given domains. For the simplest situation, that of simply connected domains, the problem of finding a single mapping is clarified by the following well-known result.

Theorem 1. *RIEMANN MAPPING THEOREM: There exists a conformal mapping f from the unit disk $\mathbb{D} = \{z\colon |z| < 1\}$ to any simply connected proper subdomain D of the complex plane (it is unique if suitably normalized).*

Knowing that a conformal mapping exists is not the same as knowing how to solve the numerical problem: given D, to calculate f to a given degree of accuracy. In some simple cases the conformal mapping can be written as a composition of elementary functions, such as Möbius transformations, powers

and roots, trigonometric functions, elliptic integrals, and the like. These basic analytic formulas are also useful for reducing general problems to more accessible ones (see Section 6.2 below). In practice, a mapping problem can be presented in a variety of ways, partly because a domain can be presented in a variety of ways: as set of points satisfying a certain condition (such as an inequality $F(z) < c$), or a specific list of points (such as a set of pixels in an image). More commonly, a domain is specified in terms of its boundary, which may be a condition satisfied by its points (such as an equality $F(z) = c$), or a parametrization $z = \gamma(t)$, or simply a list of points along the boundary.

Furthermore, a map from one domain D_1 to D_2 is often described as a composition of a map from $\mathbb{D}$ to D_1 composed with the inverse of a map from $\mathbb{D}$ to D_2. Depending on the nature of the numerical description, it may be difficult or inconvenient to calculate the inverse map.

The following result is also relevant to numerical work.

Theorem 2. *(Carathéodory) Every conformal mapping between to Jordan regions extends to a homeomorphism of the closures of the regions.*

Because of the Cauchy Integral Formula

$$f(z_0) = \int_{\partial\mathbb{D}} \frac{f(z)}{z - z_0} dz, \ z_0 \in \mathbb{D}, \tag{1}$$

which is valid for analytic functions in $\mathbb{D}$ continuous on the boundary, *it is sufficient to know the values of a conformal mapping on the boundary of* $\mathbb{D}$. This observation reduces the complexity of the conformal mapping problem from 2

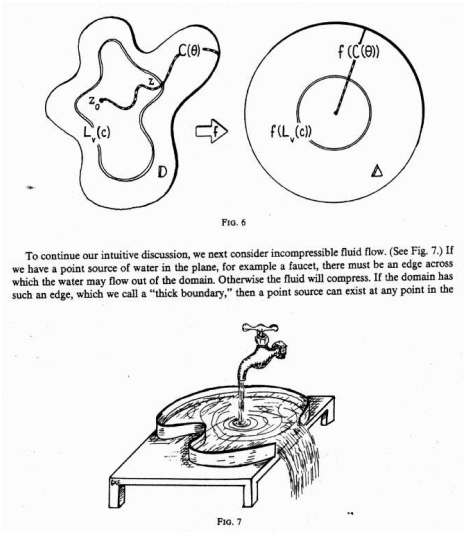

Given data:
(i) D (or ∂D)
(ii) $z_0 \in D$

FIGURE 10. Illustration by G. Francis in [1]. Equipotential lines of ideal fluid flow correspond to concentric circles under Riemann mapping.

dimensions to 1, and this is why the vast majority of the numerical methods which have been developed focus on calculating the boundary mapping $f|_{\partial\mathbb{D}}$. A numerical scheme for evaluating (1), once the boundary mapping is known, can be found in [12].

For this reason, we will consider the problem as defined in Figure 11 (except for Section 6, where the inverse mapping will be sought). The closed curve $t \mapsto \gamma(t)$ defines the boundary of D. A point z_0 fixed inside of γ is to be equal to $f(0)$. We are interested in the boundary values $f(e^{i\theta})$ for $0 \leq \theta < 2\pi$. The mapping $\theta \mapsto e^{i\theta}$ of the interval to the unit circumference is so natural that we use it in the statement of the problem: to find a function $t = b(\theta)$ so that

$$f(e^{i\theta}) = \gamma(b(\theta)). \tag{2}$$

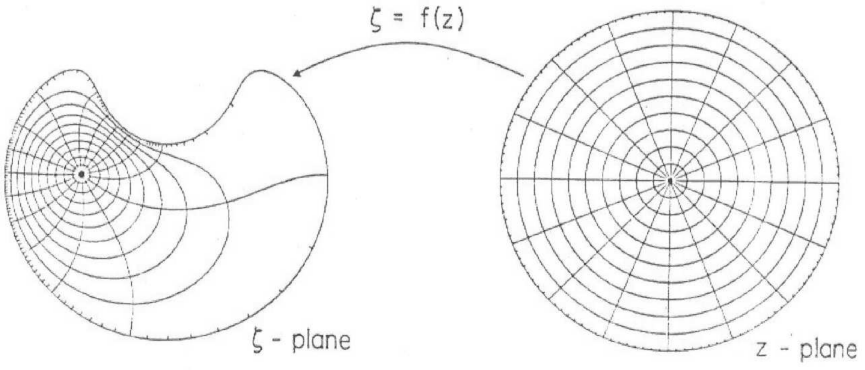

FIG 1. *Example of conformal mapping.*

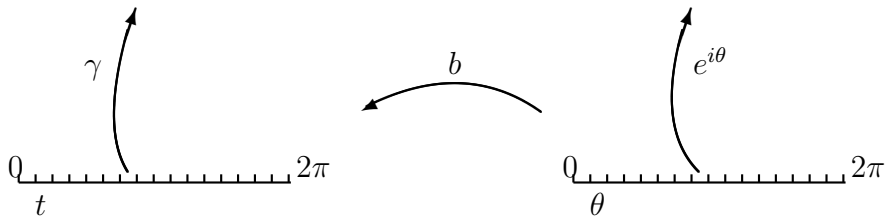

FIGURE 11. Elements of mapping problem (picture taken from [8])

4. The Crowding Problem

When f is a conformal mapping, the value of $|f'|$ (or the density of the grid points required) may vary greatly along different parts of the boundary. The *crowding factor* is the ratio of the greatest to the least value of $|f'|$. For example, consider conformal maps f_a from $\mathbb{D}$ (or from a square, as in Figure 12) to rectangles of height 1 and base $a > 0$, with $f_a(0)$ at the center of the rectangle. Then the crowding factor grows exponentially with a as $a \to \infty$.

This creates a numerical difficulty. Suppose we have calculated $b(2\pi j/N)$ for $j = 1, \ldots, N$, that is, for N equally spaced values of θ. If the crowding factor

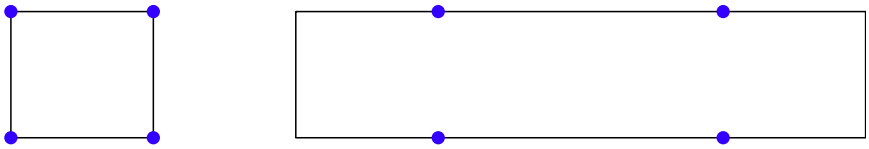

FIGURE 12. Conformal maps between non-similar rectangles cannot send vertices to vertices.

is very large, then many of these values will be bunched together, while other points will be spread relatively far apart. This may cause an imperfect picture of the behavior the mapping function (see for example the last picture in Figure 29 below). The crowding factor for the domain in Figure 11 is approximately 1000.

5. Elementary Facts about Analytic Functions

There are a great many theorems in Complex Analysis of the form "the function f is analytic if and only if ...". A conformal mapping is the same thing as a 1-to-1 analytic function, and this notion also admits many characterizations.

Theorem 3. *An analytic and 1-to-1 function $f : D \to \mathbb{D}$ is* onto $\mathbb{D}$ *when $|f'(z_0)|$ is maximal among the class of injective analytic functions $D \to \mathbb{D}$ sending the point z_0 to 0.*

Likewise there are many characterizations of boundary values on $\partial\mathbb{D} = \{|z| = 1\}$ for conformal mappings. We list without detailed explanations, a few which have been used as the basis for numerical methods.

Theorem 4. *A continuous function $\gamma\colon \partial\mathbb{D} \to \mathbb{C}$ is the boundary value of an analytic function if:*

1. [12] $\mathcal{K}[\operatorname{Re}\gamma] = \operatorname{Im}\gamma$, *where $\mathcal{K}$ is the conjugate boundary operator;*
   or if
2. [8] *its Fourier series $\gamma(t) = \sum_{-\infty}^{\infty} b_k e^{kit}$ has $b_k = 0$ for $k < 0$;*
   or if
3. [17],[22] $|\gamma'(t)|^{1/2} S(\gamma(t), z_0) + \int_0^\beta |\gamma'(t)|^{1/2} A(\gamma(t), \gamma(s)) |\gamma'(s)|^{1/2}$
   $= |\gamma'(t)|^{1/2} \overline{H(z_0, \gamma(t))}$,
   where A and H are the Kerzman-Stein and the Cauchy kernels;
   or if
4. *etc., etc.*

Generally speaking, we may say that each theoretical characterization of conformal mappings can lead to a numerical method or to a family of numerical methods. At the risk of oversimplifying, we can say that most methods fall into one of the following two classes.

- "Easy Methods": $D \to \mathbb{D}$
- "Fast Methods": $\mathbb{D} \to D$

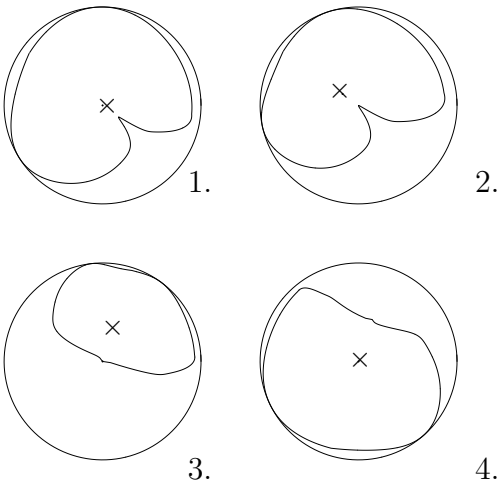

FIGURE 13. One iteration of the Koebe square-root method

We give some illustrations below.

6. Osculation Methods

Most of the "Easy Methods" are classified as *osculation methods*, which consist of first mapping D *into* $\mathbb{D}$, and then mapping the image region to a larger region inside of $\mathbb{D}$, and so on. The desired approximation to $f : D \to \mathbb{D}$ is the composition of these mappings, and f itself is their limit.

6.1. Koebe's method. The first osculation method ever created is based on the proof given by P. Koebe in 1905 for Theorem 3, and which is found in many Complex Variables texts, such as [2], [5]. This procedure is illustrated in Figure 13. The steps are prescribed as follows.

0. Suppose $D \subset \mathbb{D}$

1. Find t_0 with $|\gamma(t_0)| < 1$ minimal ("worst boundary point"). Let $a_0 = \gamma(t_0)$

2. Move a_0 to 0: $w_1 = \dfrac{w - a_0}{1 - \overline{a_0} w}$

3. Take square root: $w_2 = \sqrt{w_1}$

4. Move the image b_0 of zero back to 0:
$$w = \frac{w_2 - b_0}{1 - \overline{b_0} w_2}$$

The auxiliary mappings defined in steps 2, 3, and 4 combine to give a map from $\mathbb{D}$ to itself which fixes the origin and has derivative greater than 1. Thus

the image under each successive iteration is "larger" than the previous one. Note that if $D = \mathbb{D}$, then step 2 cannot be applied.

The images of a domain under successive iterations of the Koebe method are shown in Figure 14. The convergence to ∂D can be made slightly faster by using the cube root instead of the square root in Step 3. If one uses the nth root and lets $n \to \infty$, one approaches the *Koebe logarithm method*, in which the logarithm replaces the nth root and step 4 is modified accordingly.

6.2. Graphical methods. In the 1950's, people were looking for ways to find a mapping of a given domain to a domain reasonably close to $\mathbb{D}$, in order to apply then a fast method (such as Teodorsen's method below) to the result. Today it seems incredible that this was done by hand. For example, in [11] a method was described by which the operator first fits manually the given domain D into a disk from which a sector bounded by two arcs has been removed (Figure 15). A conformal mapping from this slightly larger domain $D_1 \supset D$ to $\mathbb{D}$ can be written in elementary terms,

$$\frac{c + z_1}{c - z_1} = k \left(\frac{c + z}{c - z} \right)^{1/\alpha}. \tag{3}$$

as a composition of a power function with two Möbius transformations. These Möbius transformations make the points $0, \infty$ correspond to key points in the original figure. An ingenious scheme was presented in which one places the domain over specially designed "graph paper" showing circles passing through

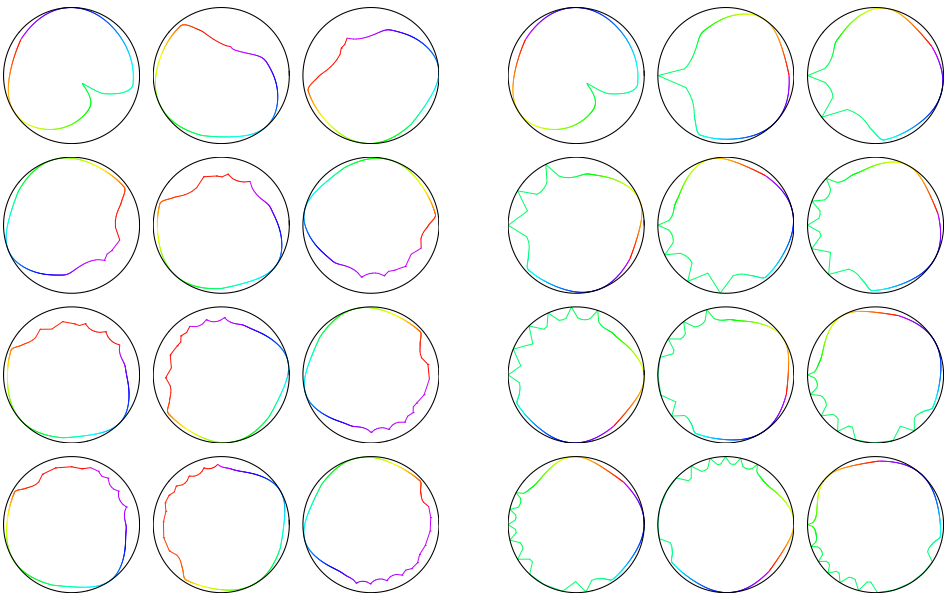

FIGURE 14. Iterations of the Koebe method (left) and the logarithmic Koebe method (right)

these two points and circles orthogonal to them. Then, much in the way that one can magnify a picture by tracing a grid over it and then copying the part of the picture in each small square in it to the corresponding square in a larger grid, pieces of the boundary of the domain are copied to corresponding pieces within a second graph paper. In this way the conformal mapping is approximated without computing the elements of (3) numerically.

6.3. Grassmann's method. In 1979, E. Grassmann [10] automated and refined this idea of Albrecht-Heinhold, giving a much faster osculation method. The first step is to detect automatically (that is, by a computer program) whether an auxiliary mapping which opens a slit can be applied, and if not, applies other alternatives. In the worst case, the Koebe method is used (Figure 16). The idea behind this method is that for many domains, after a few iterations the domain is "opened up" sufficiently so that the better auxiliary mappings will be applicable.

6.4. Sinh-log method. This method is based on the observation [19] that in the logarithmic Koebe method, at a certain step during each iteration, the logarithmic image of the domain generally not only lies in the left half-plane, but within some horizontal band; that is, the imaginary parts of all its points are bounded above and below. An appropriate real-affine transformation takes this half-band to the normalized half-band $\{-\pi/2 < \operatorname{Im} z < \pi/2\}$, which in turn the hyperbolic sine function sends to the whole left half-plane, as shown in Figure 17. As a result, a much larger part of the half-plane is covered before the half-plane is mapped back to the unit disk in the last step of the iterative procedure.

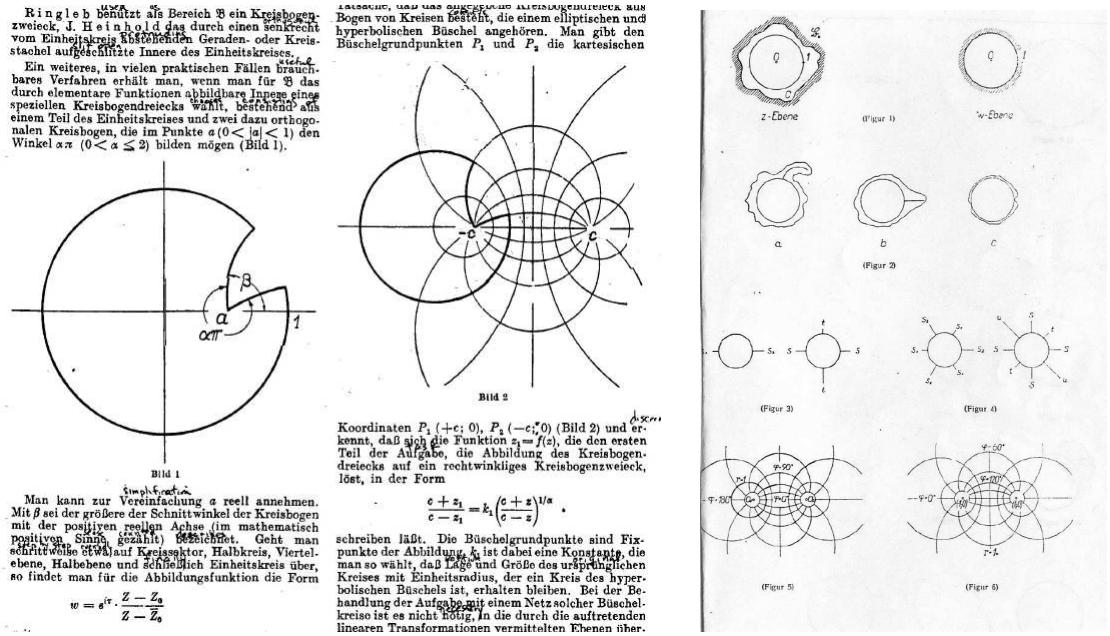

FIGURE 15. Manual graphical approach of Albrecht and Heinhold

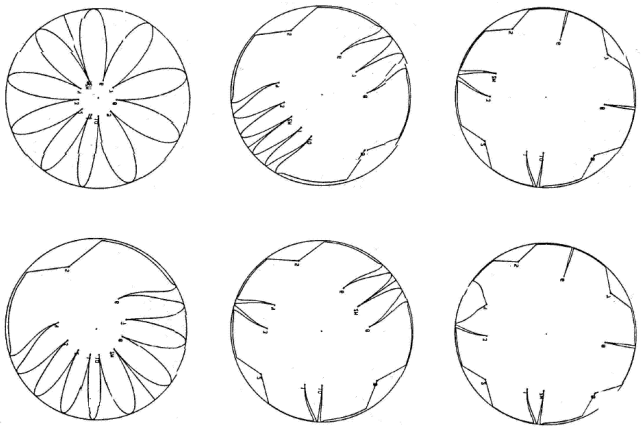

FIGURE 16. Application of Grassmann's method to a "daisy" domain. Each figure shows the slit which is opened to form the following one.

Thus the "sinh-log" method is defined by following steps 0, 1, and 2 of the Koebe square-root algorithm, then (3) taking the logarithm of the resulting image; (4) applying an affine transformation to a subdomain of the normalized half-band; (5) applying sinh, and finally (6) a Möbius transformation of the left half-plane to $\mathbb{D}$ so that the composition of all the maps mentioned fixes the origin.

The sinh-log algorithm converges roughly as does Grassmann's for many standard domains and for highly irregular domains it performs much better, while being easier to program and more stable numerically. In particular, if one is interested in calculating the composed mapping f and its inverse, it is easier to save the data for a sequence of elementary maps of a single kind.

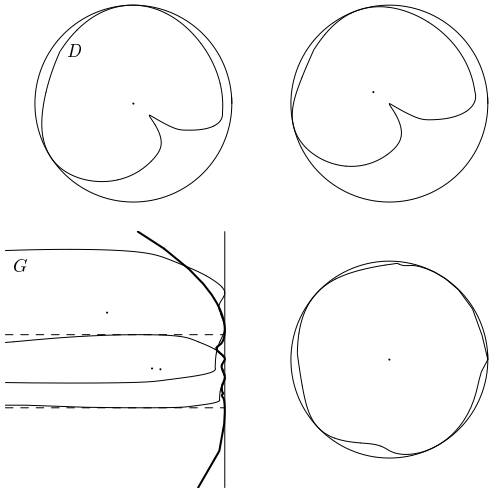

FIGURE 17. One iteration of the sinh-log method. The lower left picture shows the half-strip containing the logarithmic image, as well as the image of this under sinh

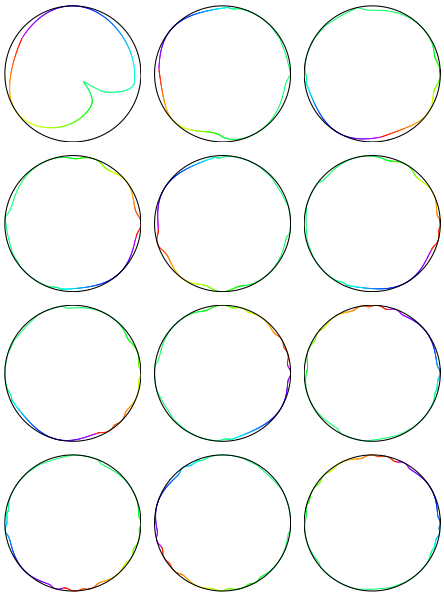

FIGURE 18. Iterations of the sinh-log method

It was mentioned that osculations are very "slow" methods. Their great advantage is that they apply to any domain bounded by a continuous (say piecewise smooth) closed curve. In general, osculation methods have the following characteristics.

Osculation Methods
COST OF ONE ITERATION: $O(N)$
RATE OF CONVERGENCE: *very slow*
GENERALITY: *total*

7. Schwarz-Christoffel Methods

The *Schwarz-Christoffel methods* are applicable to the particular case of a domain with polygonal boundary. Although for numerical work every domain can be considered in principle "polygonal," if the number of vertices is extremely large the advantage of Schwarz-Christoffel methods would be lost. The Schwarz-Christoffel formula says that the Riemann mapping from the unit disk to a polygonal domain is equal to the integral

$$f(z) = \int_0^z \frac{dz}{(z-z_1)^{1-\alpha_1/\pi}(z-z_2)^{1-\alpha_2/\pi}\cdots(z-z_n)^{1-\alpha_n/\pi}}. \tag{4}$$

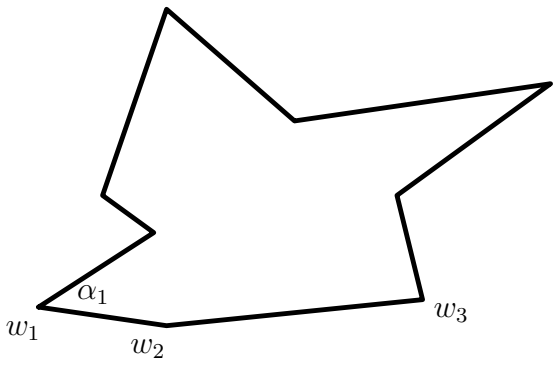

FIGURE 19

For a given polygonal domain, the vertices $w_j = f(z_j)$ are known as well as are the interior angles $\pi\alpha_j$, but the prevertices z_j are not known, so formula (4) is useless until these values are determined. A strategy for a typical Schwarz-Christoffel method would thus be

- guess approximate values for $z_1, z_2, ...,$
- evaluate the Schwarz-Christoffel integral,
- compare the results with $w_1, w_2, ...,$
- apply some type of correction

The difficulty is to make an initial guess sufficiently close for this to work. A history and detailed explanation of various methods can be found in [6]. An elegant solution to the Schwarz-Christoffel mapping question was invented by T. A. Driscoll and S. A. Vavasis [7], which begins by triangulating the polygonal domain in a special way, and then solving a set of equations for the cross ratios of all rectangles formed by pairs of adjacent triangles. Not only is there no problem to find an appropriate initial guess, but also the invariance of the cross ratio makes it possible to avoid the crowding phenomenon: one can apply a Möbius transformation of $\mathbb{D}$ to bring any part of the domain into focus.

8. Rapidly Converging Methods

It must be stressed that we will mention only a few of the very many methods which have been developed. Details and history of many classical methods will be found in [12]; for more methods see Section 13.

8.1. Theodorsen's Method. This method, presented in 1931 for improving the design of aircraft wings, applies only to starshaped domains (λz is in D when z is in D and $0 < \lambda < 1$). The region exterior to an airplane wing, in which the physics of air movement takes place, is obviously not of this form, but can be reduced to it by a suitable auxiliary transformation (Joukowski profile, Figure 21).

So we assume from the start that the boundary ∂D is traced out by

$$\gamma(t) = \rho(t)e^{it},\ 0 \le t \le 2\pi. \tag{5}$$

The idea behind the algorithm is that of condition 1 in Theorem 4. Consider the real and imaginary parts u,v of the analytic function $f(z) = u(z) + iv(z)$. They are known to be *harmonic conjugates*. Now if we are given a function u_0 defined only on $\partial\mathbb{D}$, it can be extended (by the Poisson integral) to a harmonic function u in all of $\mathbb{D}$. This function has a harmonic conjugate v defined in $\partial\mathbb{D}$. The restriction v_0 of v to $\partial\mathbb{D}$ is called the *conjugate boundary function* of u_0, and is written

$$\mathcal{K}[u_0] = v_0. \tag{6}$$

Now we apply the following facts.

1. The conjugate boundary function can be calculated by a singular integral
$$\mathcal{K}[v_0](e^{it}) = \int_0^{2\pi} v_0(e^{is}) \cot \frac{t-s}{2}\, ds.$$
2. If $\gamma(b(\theta)) = u_0(e^{i\theta}) + iv_0(e^{i\theta})$ and if $v_0 = \mathcal{K}[u_0]$, then $\gamma \circ b$ defines the boundary values of a conformal map.

Recall from Section 3 that we want $t = b(\theta)$ such that $\gamma(b(\theta))$ defines the boundary values of an analytic function according to (2). This is equivalent to

$$b(\theta) - \theta = \mathcal{K}[\log(\rho \circ b)](\theta).$$

The difference $\delta(\theta) = b(\theta) - \theta$ satisfies

$$\delta(\theta) = \mathcal{K}[\log(\rho(\theta + \delta(\theta))]. \tag{7}$$

Thus δ is a fixed point of a nonlinear operator, and Theodorsen's method says to construct a sequence of functions by iterating it,

$$\delta_{k+1}(\theta) = \mathcal{K}[\,\log(\rho(\theta + \delta_k(\theta)))\,].$$

Then $\delta_k \to \delta$ as $k \to \infty$. The solution b is now given by $b(\theta) = \theta + \delta(\theta)$.

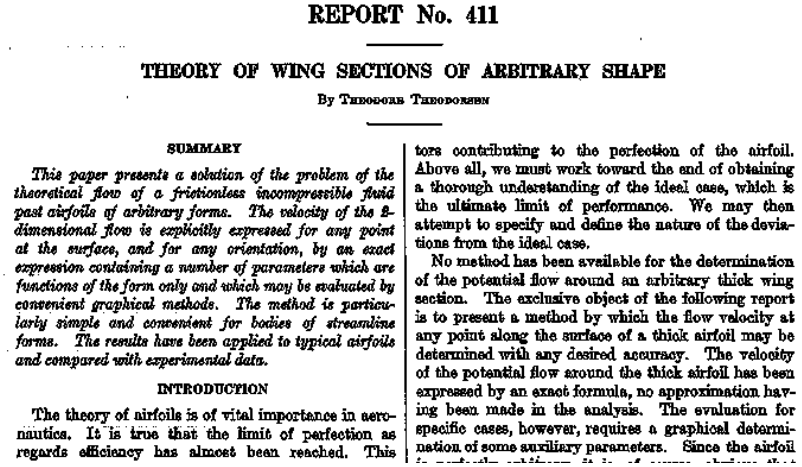

REPORT No. 411

THEORY OF WING SECTIONS OF ARBITRARY SHAPE

By Theodore Theodorsen

SUMMARY

This paper presents a solution of the problem of the theoretical flow of a frictionless incompressible fluid past airfoils of arbitrary forms. The velocity of the 2-dimensional flow is explicitly expressed for any point at the surface, and for any orientation, by an exact expression containing a number of parameters which are functions of the form only and which may be evaluated by convenient graphical methods. The method is particularly simple and convenient for bodies of streamline forms. The results have been applied to typical airfoils and compared with experimental data.

INTRODUCTION

The theory of airfoils is of vital importance in aeronautics. It is true that the limit of perfection as regards efficiency has almost been reached. This tors contributing to the perfection of the airfoil. Above all, we must work toward the end of obtaining a thorough understanding of the ideal case, which is the ultimate limit of performance. We may then attempt to specify and define the nature of the deviations from the ideal case.

No method has been available for the determination of the potential flow around an arbitrary thick wing section. The exclusive object of the following report is to present a method by which the flow velocity at any point along the surface of a thick airfoil may be determined with any desired accuracy. The velocity of the potential flow around the thick airfoil has been expressed by an exact formula, no approximation having been made in the analysis. The evaluation for specific cases, however, requires a graphical determination of some auxiliary parameters. Since the airfoil

FIGURE 20. Facsimile of Theodorsen's Naca internal report

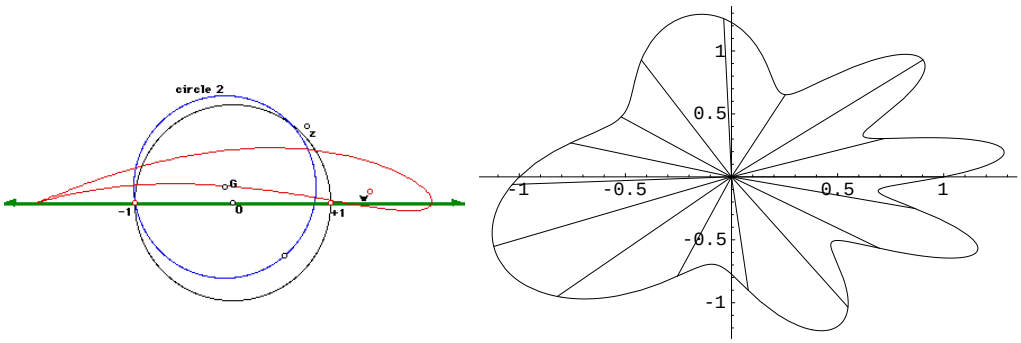

FIGURE 21. Joukowski profile and starshaped domain

Theodorsen's Method
COST OF ONE INTERATION: $O(N^2)$
RATE OF CONVERGENCE: *linear*
GENERALITY: *starshaped domain; close initial guess*

8.2. Fornberg's method. This method, published in 1980 in [8], is based on criterion 2 of Theorem 4. We have as data for the problem $\gamma : [0, 2\pi] \to \partial D$, a periodic complex-valued function, together with a point z_0 inside of D. We want to find the boundary values $\gamma \circ b$ of the conformal mapping from $\mathbb{D}$ to D sending 0 to z_0. Like any map of the circle, it must have a Fourier series:

$$\gamma(b(t)) = \sum_{k=-\infty}^{\infty} b_k e^{kit}. \tag{8}$$

From what we have said $\gamma(b(\theta))$ is to give the values on ∂D of an analytic function $f(z) = \sum_{k=0}^{\infty} a_k z^k$, so by (2)

$$\sum_{k=0}^{\infty} a_k\, e^{ki\theta} = \underline{f(e^{i\theta}) = \gamma(b(\theta))} = \sum_{k=-\infty}^{\infty} b_k\, e^{ki\theta} \tag{9}$$

and therefore

$$b_k = \begin{cases} 0, & k < 0, \\ a_k, & k \geq 0. \end{cases}$$

This suggests the following procedure.

0. Guess initial values $t_1, t_2, \ldots, t_N$ to be assigned as $b(2j\pi/N) = t_j$, i.e., we hope that $f(e^{2j\pi i/N}) = \gamma(t_j)$ approximately.
1. For b determined this way, calculate the Fourier coefficients for $\gamma \circ b$:
$$b_{-N}, b_{-(N-1)}, \ldots, b_{-1}$$
2. Calculate the corresponding changes in b_k which would go with slightly different values of t_j,
$$t_1 + \Delta t_1,\ t_2 + \Delta t_2,\ \ldots,\ t_N + \Delta t_N$$
3. Solve a linear system for the differences
$$(\Delta t_1, \Delta t_2, \ldots, \Delta t_N)$$
to make the coefficients b_k equal to zero (approximately).

Fornberg's Method
COST OF ONE ITERATION: $O(N \log N)$
RATE OF CONVERGENCE: *linear*
GENERALITY: *requires close initial solution*

9. Generalities on Conformal Mapping Methods

We have mentioned that there are a great many conformal mapping methods, each based on a specific property of functions of a complex variable. Here we have seen only a few. There are other better ones; for example, Wegmann's method [25] based on the Riemann-Hilbert problem, has the same $O(N \log N)$ iteration cost and offers quadratic convergence. We suggest the following general approach for discovering new such methods.

- Choose a characterization of analytic mapping functions
- Use it to measure in some sense how much a given function falls short of this criterion
- Write an equation to describe this numerically
- Apply some numerical method to solve this equation
- . . . and hope that it works!

10. Interpolating Polynomial Method

We describe here the method presented in [18], together with some of the ideas that led to its development, and some ideas for variations of the method. We take as the first step in our heuristic procedure the following fact proved by Wegmann [24].

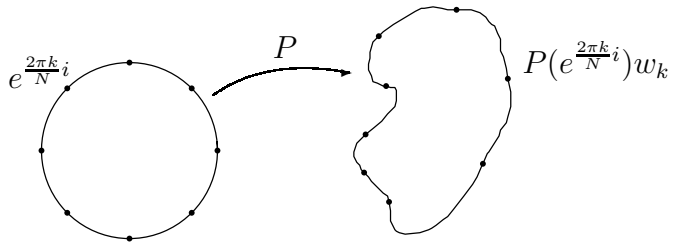

FIGURE 22. Polynomial approximation of f

Theorem 5. *For ∂D sufficiently smooth and for N sufficiently large, there is a unique (suitably normalized) polynomial of degree $N+1$ close to f which takes the $2N$-th roots of unity to points cyclicly ordered along ∂D. These polynomials approach f as $N \to \infty$.*

Let us explain what is involved in this result. Recall that our problem is to find $w_j \in \partial D$ such that $e^{2\pi ij/N} \leftrightarrow w_j$.

Consider some points $w_1, w_2, \ldots, w_N$ along ∂D. Let us investigate the hypothesis that these indeed could be the values of $f(e^{\frac{2\pi k}{N}i})$ for a Riemann mapping f from the unit disk to D.

Let us suppose that f is to be approximated by a polynomial $P(z)$ of degree N. Now, it is very easy to find a polynomial $P(z)$ such that $P(e^{j\frac{2\pi i}{N}}) = w_j$, $j = 1, \ldots, N$. Thus the existence of such a polynomial tells us nothing about whether (w_j) are the right points or not for f.

For N fixed, let us write $\zeta_j = e^{j\frac{2\pi i}{N}}$. Wegmann's theorem says that if (w_j) are the right points for f at ζ_k, then the polynomial approximation P will not only be right for f at ζ_j, but also at $\zeta_{j+\frac{1}{2}}$. For ease of reference, I will call $\zeta_{j+\frac{1}{2}}$ the "half-click" points. In Figure 23 we take $D = \mathbb{D}$, $z_0 = 0$, so that the solution is $f =$ identity (or any rotation). We have deliberately taken w_k not to be equally spaced along ∂D, and then calculated the image of all of $\partial\mathbb{D}$ under the corresponding interpolating polynomial. The images of the half-click points are marked with an $\times$.

When w_j are not the correct values for $f(\zeta_j)$, then the polynomial approximation may be very far from ∂D at the half-click points. Further, the image $P(\partial\mathbb{D})$ may not be a simple curve.

This leads us to phrase the criterion for the conformal mapping: first we discretize the problem to the N points ζ_j. Our complex-analysis criterion is

- The truncated power series of f of degree N maps all the $2N$-th roots of unity close to ∂D.

The next step in the development of our algorithm is to "measure" how much a given set of guessed points (w_j) fails to fulfill this criterion.

We choose N to be a power of 2 (to facilitate the numerical work). Given $\vec{w} = (w_j)$, there is a unique $P = P_{\vec{w}}$, the *interpolating polynomial* for $\vec{w}$, such

that

$$\begin{aligned} &P_{\vec{w}} \text{ is a polynomial of degree} \le N, \\ &P_{\vec{w}}(0) = 0, \\ &P_{\vec{w}}(e^{\frac{2\pi i}{N}j}) = w_j \text{ for } 0 \le j \le N-1. \end{aligned} \tag{10}$$

Since P is easy to calculate, so are its half-click values

$$u_j = P_{\vec{w}}\left(e^{\frac{2\pi i}{N}(j+\frac{1}{2})}\right). \tag{11}$$

The answer is given by a matrix multiplication,

$$\vec{u} = C\vec{w}, \tag{12}$$

where

$$\begin{aligned} c_j &= \frac{-1}{N} + \frac{i}{N}\cot(\frac{\pi}{N}(j+\frac{1}{2})), \\ C_{jk} &= c_{j-k}). \end{aligned} \tag{13}$$

C is a *circulant matrix*, and $C\vec{w}$ can be calculated via Fast Fourier Transform (FFT) in $O(N \log N)$ operations. This is also a key feature of Fornberg's method.

10.1. Some properties of the half-click mapping. C is an orthogonal matrix, and satisfies

$$\begin{aligned} C^2 &= E = \text{shift left by one index}, \\ C &= R^{[1/2]}, \\ E &= R^{[1]} \end{aligned}$$

where

$$R^{[\beta]}(w) = w^{[\beta]} = (P_{\vec{w}}(e^{i\beta}e^{j\frac{2\pi i}{N}}))_{j=0,\ldots,N-1}.$$

By analogy one may call R a "β-click" of the W-values.

Thus we have $u_j = P_{\vec{w}}(w_j)$, $\vec{u} = C(\vec{w})$, $C(\vec{u}) = E(\vec{w})$, $(C(\vec{u}))_j = u_{j-1}$. With this we can measure the discrepancy of a given $\vec{w}$ from the criterion of Wegmann's theorem: define $\rho = \rho_D$ to be the projection onto the nearest point

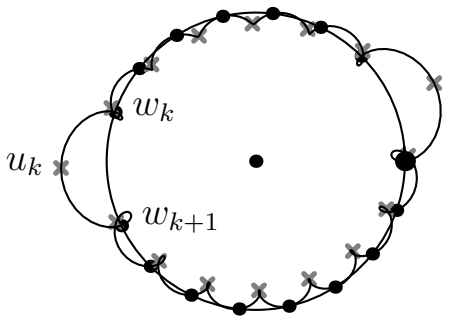

FIGURE 23. Image of $\partial\mathbb{D}$ under interpolating polynomial

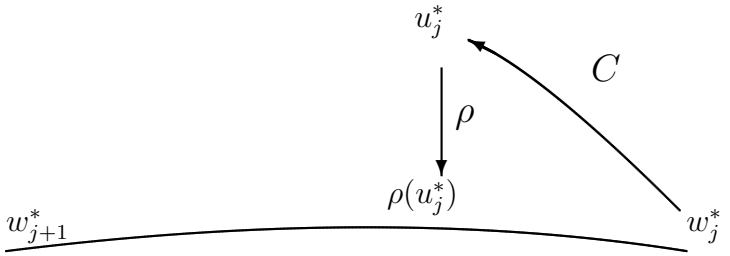

FIGURE 24. $\vec{w} \mapsto \rho(C(\vec{w}))$

of $\partial D = \gamma([0, 2\pi])$. This is defined for points sufficiently near to ∂D. Then the discrepancy can be described by the N-vector

$$(u_j - \rho(u_j))_j.$$

10.2. Interpolating polynomial algorithm. There are variations on this way of describing the discrepancy. Begin with trial values

$$\vec{w} = (w_0, w_1, \ldots, w_{N-1}) \in (\partial D)^N.$$

Calculate

$$\vec{w} \mapsto \rho(C(\vec{w})).$$

If $\vec{w}$ were the true solution, then $\rho \circ C(\vec{w})$ would be the same as $C(\vec{w}) \in \partial D$.

If we repeat the process, then the image of w_j should go over to w_{j+1}, since $C^2 = E$. This suggests looking at $\rho \circ C \circ \rho \circ C$ and comparing it with the shift E. We define the basic step of the algorithm as something very similar, and even more convenient:

$$\Phi = \Phi_D = \rho \circ C^{-1} \circ \rho \circ C \tag{14}$$

When $(\vec{w})$ is a fixed point of Φ, it follows that $\rho(u_j) = u_j$, so $u_j \in \partial D$ as required.

The numerical method for solving $\Phi(\vec{w}) = \vec{w}$, as it was in Theodorsen's method, is simply by iteration towards an attractive fixed point. When the original $\vec{w}^*$ is close enough to ∂D, the convergence to a fixed point of Φ is generally linear.

To see more clearly why "ρC" appears twice in the definition of Φ, note that the space of solutions normalized by $f(0) = 0$ can be identified with the circle S^1, being formed of

$$f_\beta(z) = f(e^{i\beta} z), \quad 0 \le \beta < 2\pi.$$

We can think of $\vec{w} = (w_0, w_1, \ldots, w_{N-1})$ being shifted (or rotated) along ∂D to $\vec{w}^{[\beta]} = (w_0^{[\beta]}, w_1^{[\beta]}, \ldots, w_{N-1}^{[\beta]})$. The "$\rho C$" algorithm approaches this *space* of solutions, but not a particular solution.

The convergence characteristics of the Interpolating Polynomial method are the same as for Fornberg's. Recall that we have fixed N, and Φ depends upon N. Therefore a solution of $\Phi(\vec{w}) = \vec{w}$ is not a true solution of the mapping problem, but rather a solution to the *truncated* problem for N-th degree. A true

algorithm for approximating the Riemann mapping to arbitrary accuracy would have to involve a step for increasing the value of N at appropriate moments.

10.3. Numerical example. For the first example, we will calculate the same Riemann mapping as did Fornberg in 1980. His domain D_α, shown in Figure 25, is bounded by the curve

$$((\text{Re } w - .5)^2 + (\text{Im } w - \alpha)^2)(1 - (\text{Re } w - .5)^2 - (\text{Im } w)^2) - 1 \;=\; 0 \tag{15}$$

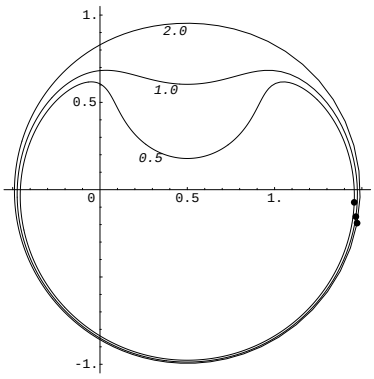

FIGURE 25. Domain defined by equation (15) for $\alpha = 0.5, 1.0, 2.0$

α	N	Iterating Φ_γ: FFTs	$\|\Delta\vec{w}\|_\infty$	$\|\Delta\vec{a}\|_\infty$	Method of Fornberg: FFTs	Accuracy of Taylor coefs.
2.0	4	16	$.48\times10^{-1}$			
2.0	8	4	$.89\times10^{-1}$			
2.0	16	4	$.16\times10^{-1}$			
2.0	32	4	$.18\times10^{-2}$			
2.0	64	8	$.91\times10^{-5}$			
2.0	128	0	—			
1.5	128	24	$.13\times10^{-8}$	$.70\times10^{-9}$	96	$.14\times10^{-7}$
1.2	128	36	$.45\times10^{-8}$	$.37\times10^{-9}$	100	$.33\times10^{-5}$
1.2	256	0	—		50	$.97\times10^{-8}$
1.0	256	48	$.68\times10^{-7}$	$.63\times10^{-8}$	108	$.17\times10^{-5}$
1.0	512	0	—		50	$.40\times10^{-8}$
.9	512	44	$.53\times10^{-7}$	$.82\times10^{-8}$	116	$.26\times10^{-6}$
.9	1024	0	—		89	$.98\times10^{-10}$
.8	1024	80	$.35\times10^{-8}$	$.33\times10^{-9}$	155	$.42\times10^{-7}$
.8	2048	0	—		81	$.55\times10^{-11}$
.75	2048	112	$.41\times10^{-9}$	$.37\times10^{-10}$	143	$.58\times10^{-9}$
.72	2048	108	$.40\times10^{-8}$	$.35\times10^{-9}$	151	$.40\times10^{-8}$
.7	2048	108	$.95\times10^{-8}$	$.81\times10^{-9}$	120	$.30\times10^{-7}$
.7	4096	0	—		81	$.31\times10^{-11}$
.68	4096	148	$.12\times10^{-9}$	$.97\times10^{-11}$	151	$.38\times10^{-10}$
.66	4096	148	$.53\times10^{-9}$	$.42\times10^{-10}$	151	$.13\times10^{-9}$
.64	4096	136	$.92\times10^{-8}$	$.69\times10^{-9}$	159	$.29\times10^{-8}$
.62	4096	136	$.33\times10^{-7}$	$.23\times10^{-8}$	140	$.19\times10^{-7}$
.6	4096	144	$.48\times10^{-7}$	$.33\times10^{-8}$	148	$.84\times10^{-7}$
.6	8192	0	—		93	$.23\times10^{-10}$
.58	8192	168	$.19\times10^{-7}$	$.12\times10^{-8}$	167	$.78\times10^{-9}$
.56	8192	188	$.14\times10^{-7}$	$.83\times10^{-9}$	171	$.90\times10^{-9}$
.54	8192	180	$.11\times10^{-6}$	$.63\times10^{-8}$	171	$.22\times10^{-7}$
.54	16384	0	—		77	$.28\times10^{-10}$
.52	16384	180	$.46\times10^{-6}$	$.23\times10^{-7}$	178	$.99\times10^{-9}$
.5	16384	212	$.25\times10^{-6}$	$.11\times10^{-7}$	228	$.15\times10^{-7}$

FIGURE 26. Table of comparative behaviour of Fornberg's method and the Interpolating Polynomial method

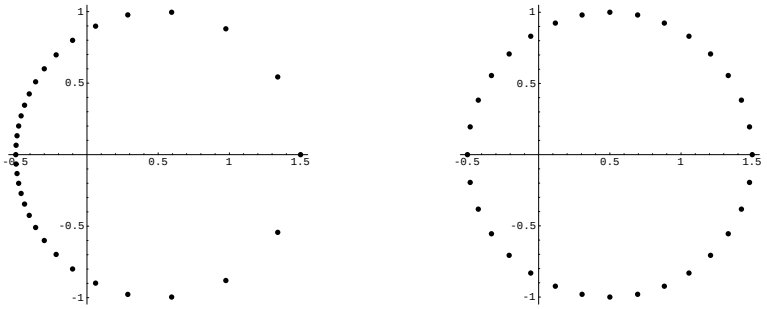

True values of $\vec{w}$ Initial test values $\vec{w}^*$

FIGURE 27.

with a variable parameter α. The high crowding factor for the domain $D_{0.5}$ mentioned earlier is largely due to the fact that the base point $z_0 = 0$ is near the left-hand side of the domain. If one starts with evenly spaced points along the boundary, then probably none of the "fast" methods will converge to the solution. In fact, one has to be extremely close to the solution for convergence to be possible. One way to get around this situation is to solve first the mapping problem for $D_{2.0}$, which is nearly circular, and then project the solution points to say, $D_{1.5}$, solve the problem there, and then project to another nearby D_α. This was done in the same way for the Interpolating Polynomial method in [18], and the fairly similar results make one wonder whether the two methods in some sense may be based on essentially the same fundamental ideas.

Now we look at a simpler domain, a unit disk which is centered at α, $0 < \alpha < 1$. The mapping function is

$$f(z) = \alpha - \frac{\alpha - z}{1 - \alpha z}. \tag{16}$$

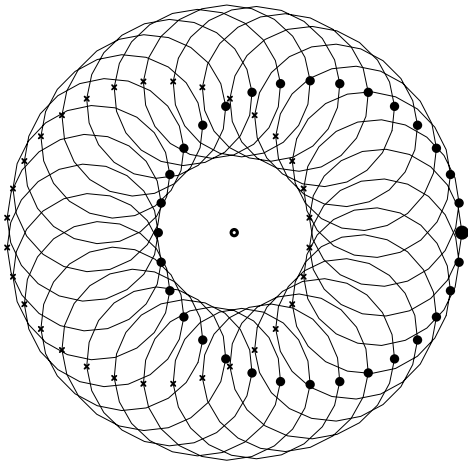

FIGURE 28. $P(\partial\mathbb{D})$ for initial test values of Figure 27

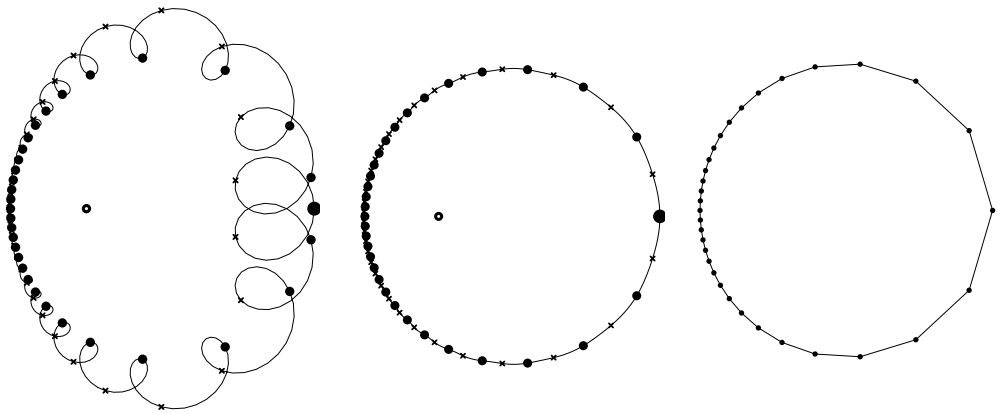

FIGURE 29. Left: $P(\partial\mathbb{D})$ after one application of the Interpolating Polynomial algorithm. Center: Result after second application. Right: Imperfect view of domain due to discretization

For illustration we take $\alpha = 0.5$ and $N = 32$. Supposing that we don't know the formula (16), we will naïvely guess that the w_j are equally spaced; i.e., we take $w_j = \zeta_j$ as on the right of Figure 27. The resulting $P(\partial\mathbb{D})$ turns out to be the rather complicated curve shown in Figure 28, a very bad approximation of the circumference of the disk.

After one iteration of Φ, a most of the w_j have moved over to the left closer to where they belong, and the image curve looks a bit more like $\partial\mathbb{D}$. At the second iteration they cannot be distinguished visually from the true positions, and the half-click images u_j appear to lie exactly on $\partial\mathbb{D}$ as well.

Of course, this is only an approximation, and to study its accuracy one may graph the change in $\vec{w}*$ from one iteration to the next. For this any convenient norm will do; in Figure 30 we use $\log||\ ||_\infty$.

In Figure 31 we show the results for 0, 1, and 2 iterations of the method for an ellipse and a square, starting in each case with equally spaced boundary points. Note that a polynomial of degree 32 does not give a particularly good approximation of the Riemann mapping for a square.

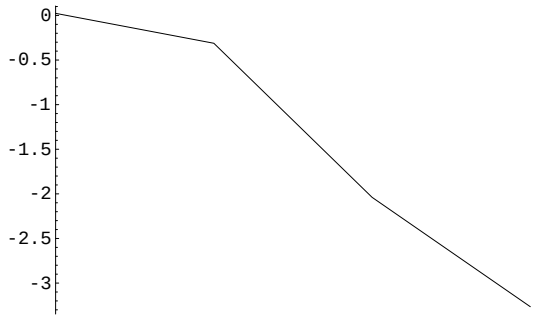

FIGURE 30. Logarithmic graph of amount $\vec{w}$ is moved in each iteration

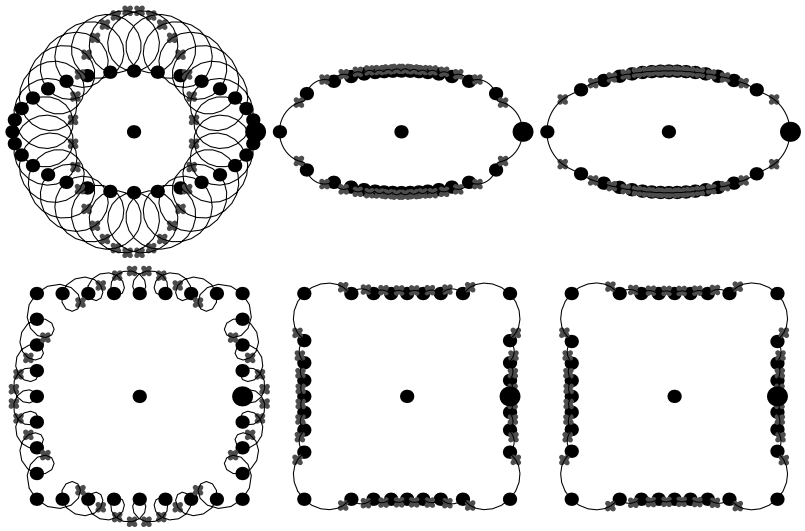

FIGURE 31. Interpolating polynomial algorithm applied to elliptical and square domains.

11. The Quest for Better Methods

Once we have the basic idea of the solution of the mapping problem being a fixed point for Φ, we can look for ways to calculate it more rapidly. Here we will describe a few attempts.

11.1. Methods using derivatives. Given $\vec{w}$ on ∂D, we can write the interpolating polynomial $P = P_{\vec{w}}$ explicitly, and thus can calculate its derivative, giving an N-vector

$$w'_j = P'_{\vec{w}}(e^{j\frac{2\pi i}{N}}) = (C'\vec{w})_j \tag{17}$$

for an appropriate matrix C'.

On the other hand, there are many other formulas involving f'. For example, from (2) we have $ie^{i\theta}f'(e^{i\theta}) = \gamma'(b(\theta))b'(\theta)$ so we can write

$$\vec{b}' = i\,\vec{\zeta}\,\frac{1}{\vec{\gamma}'}\,\vec{w}'. \tag{18}$$

Many ideas present themselves for combining (17) and (18). For example, given $\vec{b}$ one calculates $\vec{w}$ and $\vec{\gamma}'$, and then can obtain $\vec{b}'$ from which a new value of $\vec{b}$ can be estimated. Alternatively, from an initial $\vec{b}$ written as a deviation $\vec{b} = \vec{b}^* + \Delta\vec{b}$ from the true solution $\vec{b}^*$, to obtain an equation for $\Delta\vec{w}$. However, so far I have not been able to create an algorithm which converges by using any such idea.

11.2. Method of simultaneous interpolation. Let $\vec{w}^* \subseteq (\partial D)^N$ denote the true solution of the mapping problem. Let $\vec{w} \subseteq (\partial D)^N$ be an approximation. We would like to devise an algorithm which moves $\vec{w}$ closer to $\vec{w}^*$; or in other words, to calculate the difference $\Delta\vec{w}$ approximately, and then add it to $\vec{w}$ to find $\vec{w}^*$. Using the parameters $\vec{t} = (t_j) \in \mathbb{R}^N$, we see that within a neighborhood of each

$\gamma(t_j) = w_j$ the curve $\gamma = \partial D$ can be approximated by a series, which we write symbolically as

$$\gamma(\vec{t} + \Delta\vec{t}) = \vec{w} + \vec{\gamma}'\Delta\vec{t} + \frac{\vec{\gamma}''}{2}\Delta\vec{t}^{\,2} + \dots \tag{19}$$

In this formula we use coordinate-wise multiplication in a natural way, which means a subscript "j" can be applied to all the letters. In particular, we want to find the value of $\Delta\vec{t}$ for which (19) is equal to $\vec{w}^*$.

To find it, write $\vec{u} = C\vec{w}$. Then near $\rho\vec{u} = \gamma(\vec{s})$, ∂D is approximated by a similar series

$$\gamma(\vec{s} + \Delta\vec{s}) = \vec{w} + \vec{\gamma}'\Delta\rho\vec{u} + \vec{\tau}'\Delta\vec{s} + \frac{\vec{\tau}''}{2}\vec{\Delta}s^{\,2} + \dots . \tag{20}$$

By the same token, there should be a value of $\Delta\vec{s}$ for which (20) is equal to $\vec{u}^* = \rho\vec{w}^*$.

First we will examine the linear approximations obtained by truncating (19), (20):

$$\vec{w}^* = \vec{w} + \vec{\gamma}'\Delta\vec{t}\,, \quad \vec{u}^* = \rho\vec{u} + \vec{\tau}'\Delta\vec{s}$$

which are connected by the relation

$$C(\vec{w} + \vec{\gamma}'\Delta\vec{t}) = \rho\vec{u} + \vec{\tau}'\Delta\vec{s}.$$

One solves this to find that

$$\operatorname{Im}\frac{C(\vec{\gamma}'\Delta\vec{t})_j}{\tau'_j} \;=\; \operatorname{Im}\frac{\rho u_j - u_j}{\tau'_j} \tag{21}$$

since $\Delta s_j \in \mathbb{R}$. The real-linear operator

$$\Delta\vec{t} \mapsto \operatorname{Im}\frac{C(\vec{\gamma}'\Delta\vec{t})}{\tau'}$$

from $\mathbb{R}^n$ to $\mathbb{R}^n$ can be seen to have a null vector $\vec{d}$ close to $\vec{1} = (1, 1, \dots)$. It can be found by standard conjugate gradient methods, and $\Delta\vec{t} = \vec{d}$ gives an approximate solution of the mapping problem since $\rho\vec{u} = \vec{u}$ by (21).

Now we will use a quadratic approximation. The relation is

$$C(\,\vec{w} + \vec{\gamma}'\Delta\vec{t} + \frac{\vec{\gamma}''}{2}\Delta\vec{t}^{\,2}\,) = \rho\vec{u} + \vec{\tau}'\Delta\vec{s} + \frac{\vec{\tau}''}{2}\Delta\vec{s}^{\,2}.$$

From what we already know concerning the linear approximation, we may cancel several terms when this is expanded. We find thus a quadratic relation between $\Delta\vec{t}$ and $\Delta\vec{s}$. The linear system already gave an approximation for $\Delta\vec{t}$, which we substitute to solve for $\Delta\vec{s}$.

The linear and quadratic versions of "simultaneous interpolation" method give fairly good convergence, as shown in Figure 32. There are two disappointing facts. One is that we have obtained slightly better convergence at a much higher calculation cost. The other is that, according to these experiments, the quadratic method seems no better than the linear one, in spite of costing a good deal more work for each iteration.

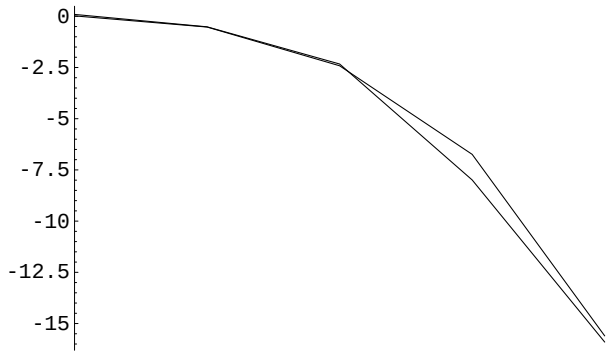

FIGURE 32.

11.3. Minimization approach. We are looking for $u_j^* \in \partial D$, so we try to minimize the quantity

$$||(I-\rho)C\vec{w}||_2^2$$

for $\vec{w} \in (\partial D)^N$. Here $||\cdot||_2$ refers to the L_2 norm. We calculate the Jacobian of the projection map at v near u. Because of the approximate relation

$$\rho v = \rho u + (u - \rho u)\ i\ \operatorname{Im}\frac{t-\rho u}{u-\rho u},$$

we find that the Jacobian mapping is

$$J_\rho(v) = \frac{1}{|a|}\begin{pmatrix} (\operatorname{Re} a)^2 & -\operatorname{Re} a\ \operatorname{Im} a \\ -\operatorname{Re} a\ \operatorname{Im} a & (\operatorname{Im} a)^2 \end{pmatrix}$$

where $a = u - \rho u$. Then the gradient of the real-valued function can be calculated to be

$$||\varphi(\vec{t})||_2^2 = ||(I-\rho)C(\vec{w}^* + \vec{\gamma}'\vec{t})||_2^2$$

which is given by

$$\begin{aligned} \nabla_{||\varphi||_2^2} &= 2J_\varphi^T\varphi \\ &= 2\ J_{\vec{\gamma}'}^T\ C^t\ J_{I-\rho}^T\ \varphi. \end{aligned}$$

Once one has the gradient, one can use it to find a value of $\Delta\vec{t}$ which minimizes the function. Some experimentation has shown that this approach works, although so far not very well.

12. Combined Methods

Recall that the "easy" methods are of general application but converge slowly, and the "fast" methods only apply when one already has a good idea of where the solution is. Thus in practice it is only logical to combine the two approaches.

Given a domain D, the first step is to map it to the interior of $\mathbb{D}$, and then apply an osculation method to obtain an image domain which is nearly circular. Then one of the faster methods can be applied to this image domain.

Figure 33, taken from [19], explains this procedure, which can be automated reasonably well. The initial domain is defined by several thousand points. The

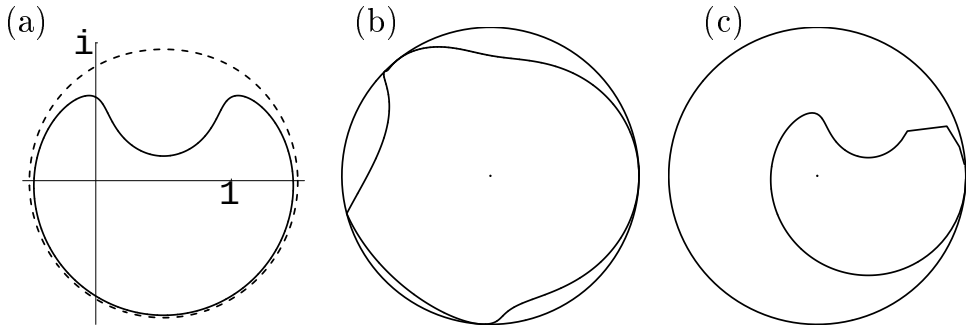

FIGURE 33. Combined method. (a) Original domain. (b) Nearly circular domain obtained by two iterations of an osculation method. (c) After applying the Interpolation Polynomial method to (b), the inverse of the osculation result is applied. Note the effect of the crowding phenomenon and discretization.

image under the osculation mapping has the same number M of points (here around 8000). The "fast" method is applied with a relatively small number N of points (here 512). This is done because the cost $O(N \log N)$ increases fairly rapidly with N. Thus when the inverse of the osculation mapping is applied, we only have N points to describe the domain. When the crowding phenomenon is present, this may cause part of the figure to be badly represented. On the other hand, if one is only interested in approximating the conformal mapping near another part of the boundary (or in the interior), this may be a very useful aspect of the method.

13. Epilogue

We suggest that the reader interested in knowing more about numerical conformal mapping consult the following.

The books [23] and [14] give detailed explanations of a great number of mappings with specific formulas. We mention also [3], a much older book, which gives a general introduction to the theory of functions of a complex variable as necessary to understand the topic of conformal mapping, as do [13], [16].

Reference [9], a half-century old text in German, is divided into two parts, covering precisely what we have called the "easy" and "fast" methods for conformal mapping. Bear in mind that the numerical examples were calculated without computers!

Reference [12] gives a much more modern and very practical treatment, including some of the methods we have described here (Koebe and Grassmann osculation, Theodorsen's method). In [15] one may find a great variety of other conformal mapping methods. As to detailed treatiseson specific methods, we recommend the book [6] on the Schwarz-Christoffel method, and [20] which explains the method of circle packings.

Finally we recommend the survey article [4], which gives a more recent perspective of the existing methods.

References

1. W. Abikoff, The uniformization theorem. *Amer. Math. Monthly* **88** (1981), 574–592.
2. L. Ahlfors, *Complex Analysis: An introduction to the theory of analytic functions of one complex variable*, Third edition, International Series in Pure and Applied Mathematics, McGraw-Hill Book Co., New York 1978.
3. L. Bieberbach, *Conformal mapping*, Chelsea, New York 1964.
4. T. K. DeLillo, *The accuracy of numerical conformal mapping methods: a survey of examples and results*, SIAM J. Numer. Anal. **31** (1994) 788–812.
5. John B. Conway, *Functions of one complex variable,* Second edition, Graduate Texts in Mathematics **11**, Springer-Verlag, New York-Berlin 1978.
6. T. A. Driscoll and L. N. Trefethen, *Schwarz-Christoffel mapping*, Cambridge Monographs on Applied and Computational Mathematics, Cambridge University Press, Cambridge 2002.
7. T. A. Driscoll and S. A. Vavasis, Numerical conformal mapping using cross-ratios and Delaunay triangulation, *SIAM J. Sci. Comput.* **19** (1998) 1783-1803.
8. B. A. Fornberg, A numerical method for conformal mapping of doubly connected regions, *SIAM J. Sci. Statist. Comput.* **5** (1984) 771–783.
9. D. Gaier, *Konstruktive Methoden der konformen Abbildung*, Springer tracts in natural philosophy, v. 3, Springer, Berlin 1964.
10. E. Grassmann, Numerical experiments with a method of successive approximation for conformal mapping. Z. Angew. Math. Phys. **30** (1979) 873–884.
11. J. Heinhold, R. Albrecht, Zur Praxis der konformen Abbildung, *Rend. Circ. Mat. Palermo* **3** (1954) 130–148.
12. P. Henrici, *Applied and computational complex analysis*, Vol. 3, Pure and Applied Mathematics (New York). A Wiley-Interscience Publication. John Wiley & Sons, Inc., New York 1986.
13. E. Hille, *Analytic function theory*, Chelsea Publishing Company, New York 1959.
14. H. Kober, *Dictionary of conformal representations*, Dover, New York 1957.
15. P. K. Kythe, *Computational conformal mapping*, Boston: Birkhüser, Boston 1998.
16. Z. Nehari, *Conformal mapping*, McGraw-Hill, New York 1952.
17. S. T. O'Donnell and V. Rokhlin, A fast algorithm for the numerical evaluation of conformal mappings, *SIAM J. Sci. Statist. Comput.* **10** (1989) 475–487.
18. R. M. Porter, An interpolating polynomial method for numerical conformal mapping. *SIAM J. Sci. Comput.* **23** (2001) 1027–1041.
19. R. M. Porter, An accelerated osculation method and its application to numerical conformal mapping, *Complex Var. Theory Appl.*, **48** (2003) 569–582.
20. K. Stephenson, *Introduction to circle packing: The theory of discrete analytic functions*, Cambridge University Press, Cambridge, 2005.
21. L. N. Trefethen and T. A. Driscoll, A. Schwarz-Christoffel mapping in the computer era. *Proceedings of the International Congress of Mathematicians, Vol. III (Berlin, 1998)*, *Doc. Math.* 1998, Extra Vol. III, 533–542.
22. M. R. Trummer, An efficient implementation of a conformal mapping method based on the szegö kernel, *SIAM J. Numer. Anal.* **23** (1986) 853–872.
23. W. von Koppenfels, *Praxis der konformen Abbildung*, Springer-Verlag, Berlin-Göttingen-Heidelberg 1959.
24. R. Wegmann, Discrete Riemann-Hilbert problems, interpolation of simply closed curves, and numerical conformal mapping, *J. Comput. Appl. Math.* **23** (1988) 323–352.

25. R. Wegmann, Conformal mapping by the method of alternating projections, *Numer. Math.* **56** (1989) 291–307.

R. Michael Porter E-MAIL: mike@math.cinvestav.mx
ADDRESS: *Department of Mathematics, Centro de Investigación y de Estudios Avanzados del I.P.N., Apdo. Postal 14-740, 07000 México, D.F., Mexico*